



**HAL**  
open science

# COMBINING MORPHOLOGICAL INTERPOLATION AND BIOMECHANICAL INVERSE KINEMATICS TO SIMULATE BIPEDAL LOCOMOTION

Nicolas Pronost, G Nicolas, G Dumont, F Multon

► **To cite this version:**

Nicolas Pronost, G Nicolas, G Dumont, F Multon. COMBINING MORPHOLOGICAL INTERPOLATION AND BIOMECHANICAL INVERSE KINEMATICS TO SIMULATE BIPEDAL LOCOMOTION. IASTED Visualization, Imaging & Image Processing (VIIP), Sep 2005, Benidorm, Spain. hal-03542823

**HAL Id: hal-03542823**

**<https://hal.science/hal-03542823>**

Submitted on 25 Jan 2022

**HAL** is a multi-disciplinary open access archive for the deposit and dissemination of scientific research documents, whether they are published or not. The documents may come from teaching and research institutions in France or abroad, or from public or private research centers.

L'archive ouverte pluridisciplinaire **HAL**, est destinée au dépôt et à la diffusion de documents scientifiques de niveau recherche, publiés ou non, émanant des établissements d'enseignement et de recherche français ou étrangers, des laboratoires publics ou privés.

# COMBINING MORPHOLOGICAL INTERPOLATION AND BIOMECHANICAL INVERSE KINEMATICS TO SIMULATE BIPEDAL LOCOMOTION

N. Pronost<sup>1\*</sup> G. Nicolas<sup>2</sup> G. Dumont<sup>1†</sup> F. Multon<sup>2</sup>

<sup>1</sup>UMR 6074 IRISA

<sup>2</sup>LPBEM

\*University of Rennes 1

University of Rennes 2

†ENS Cachan

Rennes, FRANCE

Rennes, FRANCE

email: {npronost,gdumont}@irisa.fr email: {guillaume.nicolas,Franck.Multon}@uhb.fr

## ABSTRACT

The method presented in this paper aims at calculating a plausible bipedal locomotion based on anatomical data and biomechanical locomotor hypotheses. To this end, inverse kinematics and motion interpolation are used. In classical inverse kinematics approaches, the resolution of the primary task ensures that the effector follows a given trajectory. This trajectory, considered in this work as the Cartesian displacement of the ankle as seen in the coordinate frame of the center of the pelvis, is computed using movement adaptation and interpolation in a wide database. Initially, bipedal motions are captured thanks to a motion capture system and then, mathematically modeled. After the database is built, interpolation is performed according to three locomotor constraints: step length, spacing of the feet and reference posture of the character. In this paper, we include secondary tasks that enable to take biomechanical laws for bipedal locomotion into account: respecting joint limits, resembling a given reference posture and minimizing rotational kinetic energy. A weighted sum of the resulting derivable cost functions enables us to select a specific solution in the null space of the primary task. After comparative validations related to biomechanical literature for bipedal locomotion (internal work, mechanical energy, jerk), we demonstrate that our method produces trajectories that are very close to captured ones.

## KEY WORDS

Motion retargeting, Biomechanics, Morphological and multidimensional interpolations, Inverse kinematics.

## 1 Introduction

Animating different kinds of creatures with various anthropometric properties is a difficult task given that ensuring foot contact with the ground is not enough to ensure realism. In the specific case of bipedal locomotion, several biomechanical laws were identified and enabled to produce realistic motions.

In this paper, we present a new retargeting technique based on motion interpolation in a large database. Motions

are modeled by relative displacements and are parameterized by morphological data. The adaptation is made thanks to a normalization and interpolation of these parameters. In order to recover the whole movement, we use an inverse kinematics solver, where the primary task respects the relative displacements from the adaptation and where secondary tasks ensure a realistic biomechanical movement.

Many approaches were proposed in the literature to simulate locomotion [1] that take one or several biomechanical laws into account. Among the kinematical techniques, two techniques commonly used can be put forward. The first one, called *motion editing*, consists of directly modifying motions coming from captured ones. The second one aims at solving the inverse kinematics equation by specifying constraints and helping to select one particular solution using minimization functions.

We propose to couple both inverse kinematics and motion editing in order to take those anthropometric constraints into account. With this approach, we use the main advantage of inverse kinematics where biomechanical laws enable the dealing with data directly linked to anthropometry. Motion interpolation in a database provides a plausible trajectory of the effector depending also on selected morphological parameters and locomotor hypotheses, such as the step length, the spacing between the feet and a given reference posture. We carried-out specific experiments in order to validate our approach. To this end we captured walks of 41 subjects with various morphological parameters and we compared the corresponding joint rotations to those obtained from our method.

Past works have proposed an explicit method to solve the inverse kinematics problem for limbs composed of only a few segments [2]. These methods are efficient for isolated upper and lower limbs but seem difficult to extend to a control of the whole body. Many methods can be used to solve inverse kinematics problems, and can be classified as analytic methods, numerical methods with pseudo inverse [3], or a combination of analytic and numerical methods [4]. The management of several tasks may involve conflicts which can be solved by weighing each constraint [5] or by a task-priority formulation [6][7].

Initially, trajectories of effectors can be obtained by motion capture. Retargeting is based on the adaptation of captured movements or on interpolations between these movements. Witkin et al. [8] have described a direct editing of motion curves called *motion warping*. Bruderlin and Williams [9] edited motion parameters expressed in the frequential domain. In order to apply spacetime constraints such as ensuring foot contact with the ground to a given motion, displacement maps can be added to the original angular trajectories while accounting for different morphological parameters [10]. When a constraint is lost during modification, a solver of spacetime constraints calculates an adaptation in order to restore it. The skeleton model may be improved by the addition of forces related to the muscles [11] or by physics based transformations [12]. Monzani et al. [13] proposed to use an intermediate skeleton and mix inverse kinematics and retargeting. This technique allows the conversion of movements between actors with different hierarchical models and geometrical skeletons. Savenko and Clapworthy [14] proposed an algorithm which analyzes the movement, classifies it, determines its structure, and identifies the constraints. These constraints are then used in the adaptation. The decomposition of the movement in walking cycles identifies the contact phases between the foot and the ground. This retargeting algorithm ensures that the movement is acceptable from a biomechanical point of view and corrects the possible artifacts. An alternative is to interpolate several possible locomotions using frame space interpolation [15] and motion blending [16].

This paper is organized in the following manner. Section 2 describes the representation of the lower limb used in all the paper. In section 3 we describe each step of the constitution of the motions database starting with the motion capture. Then we propose, in section 4, our interpolation method, and in section 5, we present the inverse kinematics solver used in our system. Finally we propose validations for each module developed in this paper and for the complete framework.

## 2 The hierarchical and mechanical representation of the lower-limbs chain

In this work, we focus on the simulation of the lower-limbs chain, including the pelvis. In this section, we describe a process aiming at modeling synthetic skeletons modeled with homogeneous transformation matrices thanks to anatomical descriptions. Hence, given a set of anatomical landmarks measured either on living individuals or on skeletons, we are able to construct the kinematical function that links the angular representation of the posture to the position of lower-body extremities. We choose the landmarks for their common location on living humans and on skeletons and for the facility of calculation of the articular centers which provide us our kinematical chain. This chain is composed of 5 rigid bodies, which model the limbs of

the skeleton: one pelvis, two femurs and two tibia. In this work, the feet are not included in the interpolation method but they are calculated by geometrical constraints. The root of this kinematical chain is the center of the pelvis (middle of the two Iliac spines), which can rotate about its three main axes. The pelvis is modeled as a ball and socket joint with 3 rotating degrees of freedom (denoted DOF in the remainder of the paper). Each hip is linked to the pelvis by another ball and socket joint. The knees are represented with a pin joint with one rotating DOF. More accurate articulation model could be used to take the knee into account. However, a one-DOF model is commonly used in the literature in order to animate human-like figure. We thus obtain eleven DOF for the kinematical chain presented in Figure 1. The global reference frame  $F$  is the pelvis reference frame

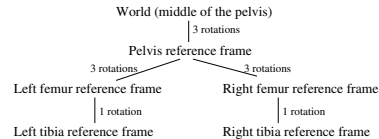


Figure 1. The hierarchical structure of the skeleton.

at the initial posture (without any rotation). Hence, the position vector  $X$  of each ankle in  $F$  is  $X = f(\{\theta\})$ , where  $\{\theta\}$  stands for the set of angles.

## 3 Motion database

In this work, the so-called *poulaine* is defined as the Cartesian displacements of the ankles as seen in the coordinate frame of the center of the pelvis (root). We choose to model this relative displacement in order to have a generic and parameterized representation of the movement. This *poulaine* is well suited to describe a walk cycle [17] and contains part of the original walking style. By modifying the *poulaine*, it is possible to adapt the gait to the target skeleton and to external constraints, by preserving the *poulaine* characteristics. Let us consider now the protocol used to capture *poulaines*.

### 3.1 Motion capture and preprocessing

We have defined a nomenclature for specific anatomical landmarks that enables us to take every kind of motion capture protocol (with different markers' placement and labeling) into account.

Specific experiments were carried-out to fill-in the database with many various *poulaines*. Gaits were captured with a motion capture system (Vicon®370, Oxford Metrics) composed of seven infrared cameras, sampled at 60Hz. According to those captured trajectories, a module extracts generic representations of the movement. In this work, this module directly calculates *poulaines*. 41 subjects participated in this experiment and walked with three

different stances: a natural walk, a bent walk and an intermediate walk.

As an output, *poulaines* and their associated speed profiles are provided but need to be modeled in order to be used by the scaling and the interpolation modules.

### 3.2 Poulaine modeling

To describe relative displacement we use the following reference frame. The center of the reference frame  $O$  is the center of the pelvis of the human (root of the skeleton), the  $\vec{x}$  axis represents the direction of displacement of the reference frame (orthogonal to the frontal plane), the  $\vec{z}$  axis represents the vertical movement of the reference frame (orthogonal to the transverse plane), and the  $\vec{y}$  axis is the vector defined such as  $(\vec{x}, \vec{y}, \vec{z})$  is an orthonormal right-handed frame (it is orthogonal to the sagittal plane). The lateral movement is represented on this axis. Although *poulaines* of very bent walks are often heterogeneous, the characteristics of their shapes are respected and we use a generic interpolation model, based on four characteristic points, to represent them. These points are associated to four precise moments of the cycle, as shown in Figure 2. Point 1 represents the moment when the ankle reaches its maximum altitude. On the curve, this point has the greatest  $\vec{z}$  component. Point 2 represents the maximum extension of the leg. On the curve, this point has the greatest  $\vec{x}$  component. Point 3 represents the moment where the ankle passes on the vertical of the root during support phase (natural stance). On the curve, this point is the point with the  $\vec{x}$  coordinate closest to 0. Point 4 represents the time of the maximum inflection of the leg. On the curve, this point has the smallest  $\vec{x}$  component. In order to interpolate the database of these relative

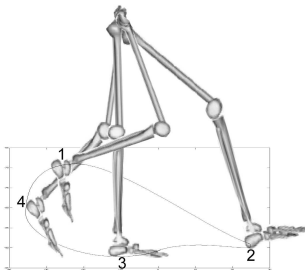


Figure 2. Positions of the four characteristic points within the cycle.

displacements, we need to model them thanks to these four specific positions. Thus the mathematical representation of a *poulaine* must be parameterized by the coordinates and must also be at least cubic for the four curves continuity. We thus chose to represent the trajectories by four cubic parameterized Coons curves, each of them defined by two of the four characteristic points and tangents. To obtain these tangents, we created an iterative algorithm, which searches for the tangents minimizing the distance between the real and the calculated curve.

After this process, we obtain the shape of the trajectories but not the speed of the effectors. To control this speed, we use an average profile computed after isolation, synchronization and normalization of walk cycles according to the duration of the steps and the size of the trajectories.

### 4 Multidimensional interpolation

The fundamental idea of our method is to separate the  $\vec{x}$ ,  $\vec{y}$  and  $\vec{z}$  interpolations and this is why we captured the walks according to the most influential parameters on each axis.

**The rest stance** of the human is associated to the  $\vec{z}$  axis, we characterize this parameter by the distance between the center of the pelvis and the ankle along this axis.

The half of the **spacing of the feet** during the support phase is associated to the  $\vec{y}$  axis. This parameter is the distance between the ankle and the walking displacement axis.

**Step length** is associated to the  $\vec{x}$  axis. This parameter is the length of the effector trace on this axis during a cycle.

Since step length characterizes the  $\vec{x}$  motion, we choose, in our set of normalized walks, the curve which has the closest step length. The  $\vec{x}$  components of coordinates and tangents of the characteristic points are stored. Since the shifting of the feet spacing during the support phase characterizes the  $\vec{y}$  motion, we choose the curve which has the closest feet spacing. The  $\vec{y}$  components of coordinates and tangents of the characteristic points are stored. Using these two interpolations, we ensure feet follow prints on the ground.

For balance reasons [17], the rest stance characterizes the  $\vec{z}$  motion. We thus select the walk which has the closest rest stance. The  $\vec{z}$  components of the coordinates and of the tangents of the characteristic points are stored. As the chosen points are only the closest approximation in our database, it is necessary to perform corrections on the obtained *poulaine*. These corrections consist of performing an exact fitting of the step length, of the foot spacing and of the stance. Furthermore, these corrections ensure that the ankle can follow the reconstructed curve. Following the obtained effector trajectory is considered as our primary task in the inverse kinematics problem. Let us consider now how we solved this problem.

### 5 Inverse kinematics with secondary tasks

We compute the Jacobian of the system according to:

$$\Delta X = J(\theta)\Delta\theta \quad (1)$$

Given a *poulaine* and an initial posture, the problem is to calculate realistic angular trajectories. The primary task is insured by inverting the previous equation. When the primary task is solved we obtain an initial value  $\Delta\theta_m$ :

$$\Delta\theta_m = J^+(\theta)\Delta X \quad (2)$$

where  $J^+$  is the pseudo-inverse of  $J$ . The solution of this equation has a minimal norm but nothing ensures that it

respects joint limits and produces realistic trajectories. To this end, a secondary task is proposed to take those constraints into account:

$$\Delta\theta = J^+(\theta)\Delta X + (I - J^+J)\delta \quad (3)$$

where  $\delta$  is the parameter to optimize and  $I$  is the diagonal unity matrix.  $\delta$  corresponds to the angle variation, which is partially realized by the projection on the null space of the linear transformation  $J$ . The second part of the equation does not modify the achievement of the primary task for any value of  $\delta$ . In order to control the movement and calculate visually realistic trajectories,  $\delta$  must verify three constraints:

- (T1) Defining a continuous and derivable cost function that rapidly increases beyond the joint limits, thanks to an exponential function:

$$f_1(\theta_t, \Delta\theta_m, \delta) = \sum_{i=1}^{11} (e^{\xi(\alpha_i - \text{bup}_i)} + e^{\xi(\text{blow}_i - \alpha_i)})$$

with  $\alpha = \theta_t + \Delta\theta_m + (I - J^+J)\delta$  (4)

where  $\theta_t$  is the current state,  $\text{bup}_i$  and  $\text{blow}_i$  are respectively the upper and the lower joint limits for the  $i^{\text{th}}$  DOF  $\theta_i$ .  $\xi$  is a constant coefficient to ensure a rapid increase when the angle is beyond the joint limits and a rapid decrease when it is within those limits.

- (T2) Minimizing the rotational kinetic energy of each body segment:

$$f_2(\theta_t, \Delta\theta_m, \delta) = \sum_{b=1}^5 \frac{1}{2} R_b I_b R_b^T (w_b((I - J^+J)\delta, \Delta\theta_m))^2 \quad (5)$$

where  $b$  stands for the body segment number,  $I_b$  is the inertia of segment  $b$  (provided by anthropometric tables).  $w_b$  is a function that computes the angular velocity vector of segment  $b$  depending on  $\Delta\theta_m$  and the optimized parameter  $\delta$ .  $R_b$  is the transform matrix between the body segment frame and the global reference frame.

- (T3) Searching a solution close to the rest posture:

$$f_3(\theta_t, \Delta\theta_m, \delta) = \|\theta_t + \Delta\theta_m + (I - J^+J)\delta - \theta_r\|^2 \quad (6)$$

where  $\theta_r$  is the angle at rest posture provided by motion capture on static trials.

We propose to use the Multidirectional Search (MDS) method [18] to solve those secondary tasks. It enables the minimization of derivable or not cost functions and is less sensitive to local minima than the steepest descent method. The global function  $z$  to optimize is  $z = f_1 + f_2 + f_3$ .

## 6 Validation and Results

In order to validate our method of adaptation by interpolations, we present a self-coherent validation where known

data are inputs and produce identical outputs. Then we show results on the coupling methods and compare them to literature and to initial data.

### 6.1 Self-coherent validation of the interpolation

The method validation step is a self-coherent validation process. We compare the produced *poulaine* for each subject to the initial one. This comparison is done in terms of shape and speed and is processed for each initial motion (a subject with a stance). The morphological and posture parameters are extracted from the skeleton model and from the motion. Let us focus, for example, on the third subject in the intermediate stance and used as input data in the proposed method. In figure 3, we compare the re-targeted *poulaine* to the captured motion of this subject. This comparison shows very few differences except for the slight shift in shape that is due to generic representation by a cubic parameterized curve. This validation was performed for all captured movements and showed the same results.

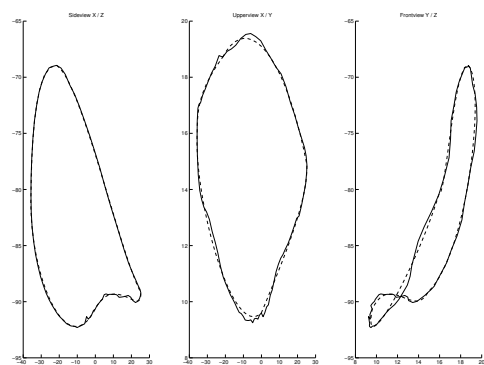


Figure 3. An initial (solid line) and reconstructed (dashed line) *poulaine* in the  $(x,z)$ ,  $(x,y)$  and  $(y,z)$  planes.

### 6.2 Results

In this section we first discuss the shape of simulated angles, compared to those classically described in literature. We then validate our model by comparing simulated angles to real angular trajectories for seven subjects.

For all subjects, simulated angles correspond to shapes classically described in biomechanical literature [17]. Let us discuss each frame of Figure 4, for subject 3. The top frame describes rotations of the pelvis. The pelvis inclination is quite constant at a value close to 0.05 rad. The pelvis obliquity is quite symmetric and range from -0.09 to 0.03 rad, as well as the pelvis internal/external rotations (range from -0.1 to 0 rad). All these values means

that the pelvis does not rotate during the walk cycle. Generally, pelvis rotations increase with the step length.

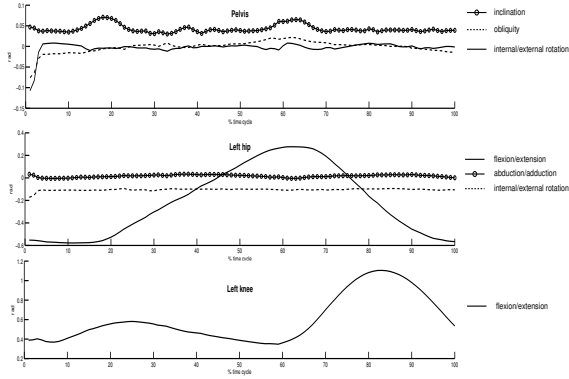


Figure 4. Simulated angles for Subject 3.

As regards with hip joint, we can observe a phase of flexion (to  $-0.58$  rad) and a phase of extension (to  $0.32$  rad). Abduction/adduction and internal/external rotations are nearly constant at a value close to  $0$  rad, which means that the movement is mainly performed in the sagittal plane.

Moreover we observe a bimodal curve for the knee angular trajectory. The first peak corresponds to heel strike on the ground, and the second part of the curve corresponds to swing phase. It is within the range  $0.35 - 1.15$  rad which is in agreement with previous biomechanical works. Finally, all the angles computed by the simulation respect the choice of joint limits.

In order to validate our model, we present simulated angles compared to real angular trajectories for seven subjects. Three-dimensional kinematics of the subject's lower extremity were documented with the Vicon370 motion analysis system. Fourteen retro-reflective markers were placed over standardized anatomical landmarks overlying the bony landmarks. We then compare the computed angles to the simulated ones in each anatomical plane. This kind of comparison is often performed in biomechanics [17].

In order to evaluate the resulting simulation, we proposed to calculate the Root Mean Square (RMS) that evaluates the difference between the simulated and the captured trajectories:

$$e_{RMS} = \sqrt{\frac{1}{T} \sum_{t=0}^T (\theta_i(t) - \hat{\theta}_i(t))^2} \quad (7)$$

where  $t$  stands for the time and  $T$  for the total duration,  $i$  for the DOF and  $\hat{\theta}_i$  for the captured trajectory. In this equation,  $\hat{\theta}_i$  is shifted to  $\theta_i$  mean value.

We also evaluate the three secondary tasks thanks to three biomechanical criteria:

- The total jerk for all the resulting sequence. Several studies in biomechanics [19] demonstrated its impor-

tance in natural human movement:

$$C_1 = \frac{1}{11} \sum_{i=1}^{11} \frac{d^3}{dt^3} \theta^2(i) \quad (8)$$

- The variation between the state vector at the last and first frames to evaluate if the sequence is cyclic:

$$C_2 = \|\theta(end) - \theta(start)\| \quad (9)$$

- The internal work calculated by an indirect method according to the kinetic energy theorem:

$$W_{int} = |\Delta[E_k] - mg\Delta h| \quad (10)$$

This method is currently used in biomechanics [20].  $E_k$  is defined as the sum of translational and rotational kinetic energies for each segment (each segment has an inertia moment given by anthropometric tables). Internal power per unit mass is then defined by:

$$C_3 = \frac{1}{mT} \sum_{t=1}^T W_{int}(t) \quad (11)$$

The results are presented in Table 1 for each subject. Mean jerk value ( $\bar{C}_1 = 7,2.10^7 rad.s^{-3}$ ) is compatible with previous biomechanical literature, for subjects walking at the same speeds [21], as well as mean internal power per unit mass ( $\bar{C}_3 = 6.1 W.kg^{-1}$ ). For some subject (for example subject 4), we can observe a weak difference between the last and the first posture that are ideally the same.

Finally, for the different joints, as those reported in Table 2, results are very close to the real trajectory. Indeed, the RMS error value between the simulated and the real angular trajectory is lower or equal to  $0.05$  rad. Figure 5 compares real angles to computed angles for subject 5, in each anatomical plane. Given that RMS errors for all pelvis DOFs are not significant, we only present angular trajectories for left hip and left knee. We obtain similar results for the right hip and the right knee.

## 7 Discussion

The method proposed in this paper is a promising alternative to dynamics simulation in order to produce plausible locomotions according to morphological parameters, such as body segments' length, mass and inertia, the shape of bones (that modifies the relative position of a joint center in its parent reference frame), the type of articulation, joint limits and a rest posture. Motion retargeting proposed in previous works generally focused on changes in body segment lengths while taking geometric constraints into account, such as ensuring foot contact. Nevertheless, joint limits and the type of articulation also act in the way motion is performed. Hence, techniques involving frame space interpolation, motion blending or statistical analyses (such as using PCA) may fail because they generally

Table 1. Criteria evaluated for seven subjects.

Subject	1	2	3	4	5	6	7	Mean value
$C_1 \times 10^7 (rad.s^{-3})$	5.2	8.7	3.6	9.2	10.3	5.2	7.9	7.2
$C_2 (rad)$	0.02	0.02	0.01	0.03	0.01	0.02	0.01	0.02
$C_3 (W.kg^{-1})$	5.1	7.2	5.7	7.1	5.6	5.9	6.1	6.1

Table 2. RMS error between the simulated and the real angular trajectories for pelvis, left hip and left knee. S.D. means standard deviation.

	pelv. incl.	pelv. obliq.	pelv. int/ext rot.	hip flex/ext	hip abd/add	hip int/ext rot.	knee flex/ext
Mean value	0.03	0.01	0.01	0.05	0.04	0.03	0.02
$\pm$ S.D (rad)	0.03	0.01	0.01	0.03	0.04	0.01	0.01

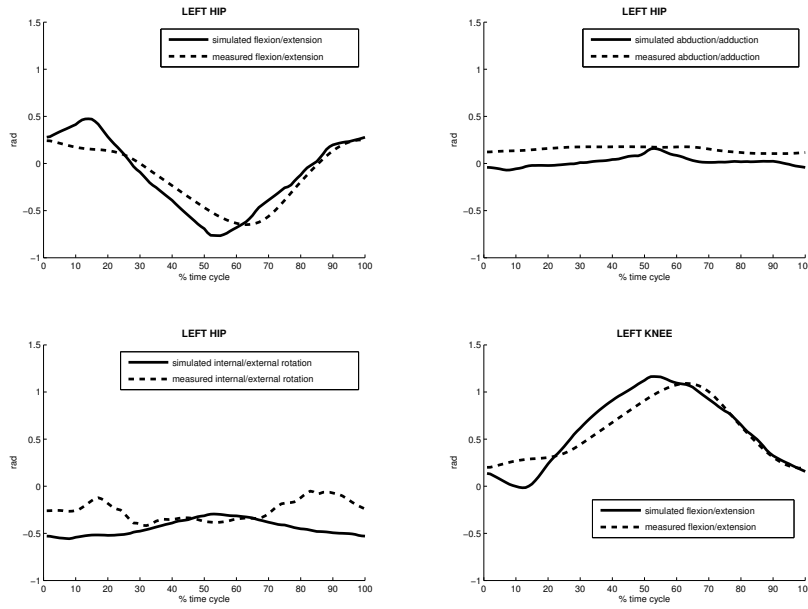


Figure 5. Simulated angles and real angles for subject 5.

assume that skeletons have a quite similar structure. Displacement maps may take this kind of parameters into account but would require application of constraints at each frame to ensure that new joint limits and bones shape are taken into account.

The database is somehow a discretization of the space representing all the possible feet movements during bipedal locomotion. To this end, a large database composed of 123 poulaines coming from 41 different subjects walking with different postures, was built. The more motions in this database, the more realistic are the motions of the feet. If no feet trajectories are stored for the kind of skeleton used in animation (such as animating a dinosaur while no motion

capture is obviously available), the system interpolates by using the skeletons that best fit to the corresponding morphological properties. If only human's feet trajectories are stored whereas a monkey must be animated, the result may be unrealistic. In future works, extrapolations driven by morphological properties should be added to this approach in order to overcome this limitation.

In this paper, we focused on the generation of plausible locomotions for bipedal human-like creatures. Specifically, we compared the simulated motions with captured trajectories. The results indicate that the simulated motions resemble real ones. This result is encouraging and demonstrates that the hypotheses used to select a specific motion

into the inverse kinematics null space are promising. This validation should be extended to other creatures that differ from humans (such as monkeys or other bipedal animals) in order to ensure that every kind of bipedal creature, even coming from fiction, can be used for the generation of plausible locomotions.

This work has several possible applications not limited to computer animation. For example, proposing plausible locomotions to fossil skeletons is an interesting field of application. In orthopaedic rehabilitation, it could also be interesting to predict locomotion adaptations due to prostheses which could be considered as morphological adaptations or after reeducation where joint limits and maximum joint angular velocity are affected.

## 8 Acknowledgments

This study was partially realized within the framework of an ATIP CNRS support: “Evaluating locomotor abilities in early hominids : 3D Modelling and simulation of Lucy’s (*Australopithecus Afarensis*) bipedalism”. This project gathers two laboratories of paleoanthropology, a laboratory of biomechanics and a laboratory of computer science.

## References

- [1] F. Multon, L. France, M. Cani-Gascuel, and G. Debunne. Computer animation of human walking: a survey. *Journal of Visualisation and Computer Animation* 10, pages 39–54, 1999.
- [2] D. Tolani and N.I. Badler. Real-time inverse kinematics of the human arm. *Presence, Teleoperators, and Virtual Environments*, 5(4):393–401, 1996.
- [3] P. Baerlocher. *Inverse kinematics techniques for the interactive posture control of articulated figures*. PhD thesis, EPFL, Switzerland, 2001.
- [4] D. Tolani, A. Goswami, and N.I. Badler. Real-time inverse kinematics techniques for anthropomorphic limbs. *Graphical Models and Image Processing*, 62-5:353–388, September 2000.
- [5] C.B. Philips, J. Zaho, and N.I. Badler. Interactive real-time articulated figure manipulation using multiple kinematic constraints. *Computer Graphics*, 24(2):245–250, 1990.
- [6] B. Le Callennec and R. Boulic. Interactive motion deformation with prioritized constraints. In DK. Pai R. Boulic, editor, *Proceedings of ACM/Eurographics SCA*, pages 163–171, Grenoble, France, august 2004.
- [7] P. Baerlocher and R. Boulic. An inverse kinematic architecture enforcing on arbitrary number of strict priority levels. *The Visual Computer*, 20(6):402–417, august 2004.
- [8] A. Witkin and Z. Popović. Motion warping. In R. Cook, editor, *Computer Graphics (Proceedings SIGGRAPH’95)*, pages 105–108, August 1995.
- [9] A. Bruderlin and L. Williams. Motion signal processing. In R. Cook, editor, *Computer Graphics SIGGRAPH’95 Proceedings*, pages 97–104, 1995.
- [10] M. Gleicher. Retargetting motion to new characters. In *SIGGRAPH’98*, 1998.
- [11] T. Komura, Y. Shinagawa, and L. Kunii. Creating and retargetting motion by the musculoskeletal human body model. *The Visual Computer*, pages 254–270, 2000.
- [12] Z. Popović and A. Witkin. Physically based motion transformation. In *SIGGRAPH’99*, 1999.
- [13] JS. Monzani, P. Baerlocher, R. Boulic, and D. Thalmann. Using an intermediate skeleton and inverse kinematics for motion retargetting. *EuroGraphics 2000*, 2000.
- [14] A. Savenko and G. Clapworthy. Using motion analysis techniques for motion retargetting. Technical report, Departement of Computer & Information Sciences - De Montfort University, 2002.
- [15] G. Ashraf and K.C. Wong. Constrained framespace interpolation. *Computer Animation 2001*, pages 61–72, 2001.
- [16] S. Park, HJ. Shin, TH. Kim, and SY. Shin. on-line motion blending for real-time locomotion generation. *Computer Animation and Virtual Worlds*, 15(3-4):125–138, July 2004.
- [17] M.W. Whittle. *Gait analysis: An introduction*. Oxford: Butterworth-Heinemann, 1991.
- [18] V. Torczon. *Multi-directional Search: A Direct Search Algorithm for Parallel Machines*. PhD thesis, Rice University, Houston, Texas, USA, 1989.
- [19] J. Laczko, S. Jaric, J. Tihanyi, V.M. Zatsiorsky, and M.L. Latash. Components of the end-effector jerk during voluntary arm movements. *Journal of Applied Biomechanics*, 16(1):14–25, 2000.
- [20] R.G. Burdett, G.S. Skrinar, and S.R. Simon. Comparison of mechanical work and metabolic energy consumption during normal gait. *Journal of Orthopaedic Research*, 1(1):63–72, 1983.
- [21] A. Hreljac and PE. Martin. The relationship between smoothness and economy during walking. *Biological Cybernetics*, 69(3):213–218, 1993.